ELSEVIER

Polymer 40 (1999) 5095–5102

polymer

High energy ion irradiation effects on polymer materials–Changes in mechanical properties of PE, PSF and PES

Tsuneo Sasuga*, Hisaaki Kudoh, Tadao Seguchi

Takasaki Radiation Chemistry Research Establishment, Japan Atomic Energy Research Institute Takasaki Gunma 370-1292, Japan

Received 7 August 1998; received in revised form 2 October 1998; accepted 9 October 1998

Abstract

The change in mechanical properties induced by irradiation of electron (2 MeV), proton (10 and 20 MeV), He^{2+} (20 and 50 MeV), and 220 MeV C^{5+} ions were studied for polymer films of polyethylene (PE), bis-phenol A based polysulphone (PSF) and polyethersulphone (PES). There is no difference between the irradiations of proton and electron in the mechanical properties for PE compared by absorbed dose. On the contrary, in aromatic polymers as PES and PSF, the decrement in the tensile strength and elongation with dose is extremely depressed in the irradiation of ion. It was found from the measurements of gel fraction and glass transition temperature that the probability of crosslinking and/or chain scission depends on linear energy transfer (LET). © 1999 Elsevier Science Ltd. All rights reserved.

Keywords: Chamber for ion irradiation; Proton and heavy ion irradiation; Dose evaluation

1. Introduction

Polymer films and fiber-reinforced plastics have been used as a thermal insulator and structural materials of artificial satellites. Not only high-energy electron but also high-energy protons and heavy ions expose materials in space environment. For the selection of materials used in such environment, the knowledge about radiation resistance against ions is very important, however, the studies in the field are few [1–8].

There are many reports that irradiation effects of organic materials are affected by energy deposition rate along the penetration depth ($-dE/dx$) of radiation source, in other words, linear energy transfer (LET) [9–21]. The LET effects on the *G*-values (chemical yield/100 eV of energy absorption) of crosslinking $G(x)$ and chain scission $G(s)$ for various polymers have been studied [14–22]. Followings are typical results in low to high energy ion irradiation: The $G(x)$ of monodisperse polystyrene (PS) irradiated by 100 keV He^+ (LET = 210 keV/μm), 200 keV Ne^+(450 keV/μm) and 400 keV Ar^+ (850 keV/μm) is 0.3, regardless of ion species and energy, but is about one order higher than the one of 0.04 in the γ-ray (LET = 0.18 keV/μm) irradiation (Calcagno and Foti et al. [14]). By the irradiation of 0.4–3 MeV H^+ (LET = 61–12 keV/μm), 0.4–3 MeV He^+ (250–160 keV/μm) and 1 MeV, N^+(620 keV/μm) $G(x)$ of monodisperse PS increases with increase of LET (Aoki et al [19]). In the irradiation of 275 MeV Ne^{7+} (430 keV/μm) and 180 MeV Ar^{8+} (2500 keV/μm) for polymetylmethacrylate (PMMA) and polymethacrylonitrile (PMAN), $G(s)$ decreases and $G(x)$ increases with increase of LET (Schnabel [18,20])

In general, it is a trend that $G(s)$ decreases and $G(x)$ increases in the high LET irradiation. These results have been interpreted in terms of increase in probability of recombination of active species creating a high density in a local area.

It is necessary in such experiments that the charged particles pass entirely through the specimen, because they deposit extremely large energy just before the end of range (Bragg peak). For this purpose, very thin specimens (0.2–0.3 μm) which are usually prepared by spin coating method, were employed in the studies using ions below MeV [14–17,19,21]. On the contrary, in the study on ion radiation-induced degradation behavior, irradiation by high energy ions is required, because usage of enough thick polymer sample (over 100 μm) is essential to obtain appropriate mechanical data. Moreover, uniform irradiation technique on wide area is indispensable for such study, but there were some difficulties in uniform irradiation of high energy ions. An ion irradiation facility (Takasaki Ion Accelerators for Advanced Radiation Application; TIARA) was constructed for research of material science in JAERI, Takasaki

* Corresponding author. Tel.: + 81-27-346-9443; fax: + 81-27-346-9687.

PII: S0032-3861(98)00725-3

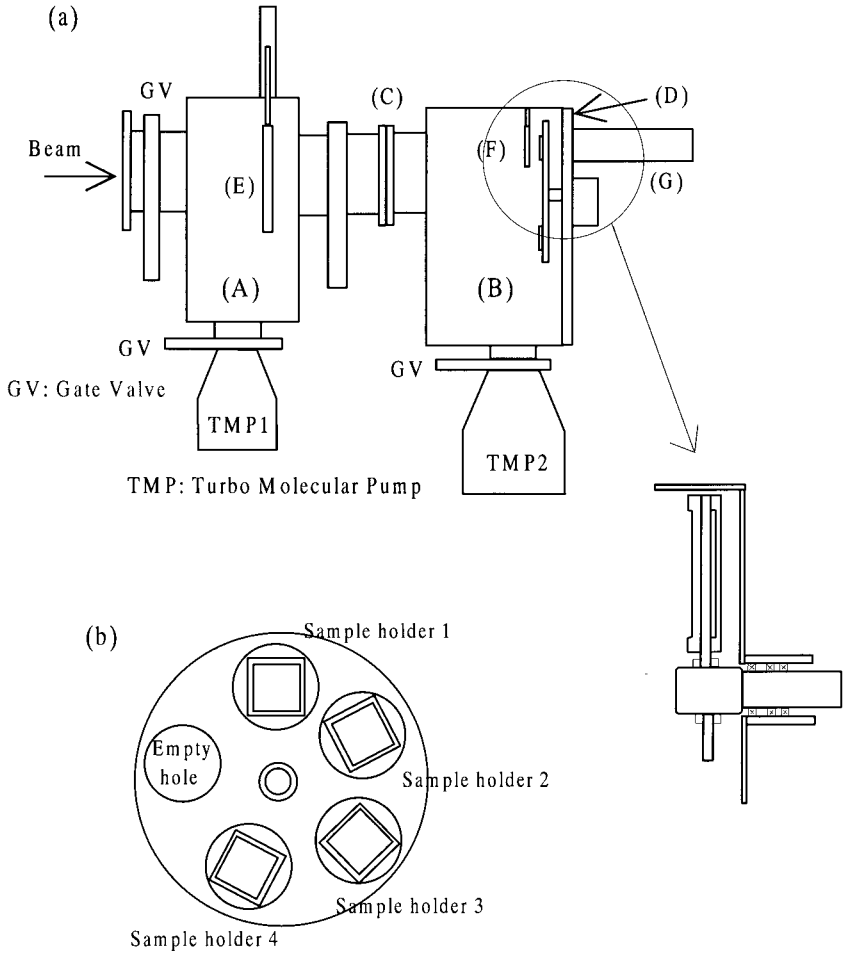

Fig. 1. Schematic draws of ion irradiation chamber (a) and sample holder module for irradiation at ambient temperature (b).

Radiation Chemistry Research Establishment [22]. AVF cyclotron in TIARA has a beam line to irradiate materials uniformly in a wide area by scanning ion beams.

Ion irradiation effects on PE, polytetrafluoroethylene (PTFE) and PMMA have been investigated by 10–45 MeV protons, 20 and 50 MeV of He^{2+}, 220 MeV C^{5+}, 100 MeV O^{5+},160 MeV O^{6+}, and 330 MeV Ar^{11+}, and it was confirmed that the radiation-induced changes in mechanical properties of these aliphatic polymers are same to those induced by 2 MeV electron and/or γ-ray irradiation [6,7] In this article, characteristic of a chamber to allow irradiation to a wide area of 100 mm × 100 mm of polymeric materials under controlled temperature and the radiation effects induced by high energy ions for one aliphatic and two aromatic polymers are reported.

2. Experimental

2.1. Chamber for uniform irradiation

A chamber as shown in Fig. 1a, schematic draws of ion irradiation chamber was constructed for ion irradiation of polymeric materials. The chamber is composed of the two vacuum vessels (high vacuum vessel (A) and irradiation vessel (B)) having individual evacuation system to keep high vacuum in beam line, because the decomposed gas are generated from polymer materials. The two vessels can be isolated from each other by inserting a thin metal foil between the two vessels in the position indicated as (C). The door (D) is the base of sample holder. By changing holder module, low and high temperature irradiations are available. The chamber has a beam shutter (E), three view ports, a gate type beam trimmer (F) and a duct type Faraday cup (G). The beam trimmer has the window of 100 mm × 100 mm size and is used to cut off the turning edge of scanning beam.

Fig. 1b shows the sample holder module for irradiation at ambient temperature. Four sample holders and one empty hole are aligned on an aluminum turret. The maximum size of irradiation area for specimen is 100 mm × 100 mm. Four specimens can be irradiated sequentially in one experiment. Graphite beam stopper and cooling water jacket are equipped just behind the each sample holder. As the turret is insulated electrically, the beam stopper plays the part of charge collector. The current of ions

Table 1
Mass stopping power and penetration range of ions for polymers

Materials	Ions and energy	Stopping power (MeV cm^2 g^{-1})	Range (mm)
Polyethylene (PE)	H^+ 10 MeV	49.5	1.16
Poly (aryl ether sulphone) (PES)	H^+ 10 MeV	42.1	0.97
	H^+ 20 MeV	24.19	3.34
	He^{2+} 50 MeV	141.1	1.45
	C^{5+} 220 MeV	927.0	0.98
Bis-phenol A based Poly (aryl sulphone) (PSF)	H^+ 10 MeV	43.6	1.03
	H^+ 20 MeV	24.83	5.59
	He^{2+} 20 MeV	306.0	0.30
	C^{5+} 220 MeV	957.0	1.05

passing through the specimen is monitored during irradiation and integrated.

2.2. Materials

Polymers were aliphatic polymer of polyethylene (PE, $d = 0.945$ g cm^{-3}) and two aromatic polymers of polyethersulphone (PES, $d = 1.37$ g cm^{-3}) and bis-phenol A based polysulphone (PSF, $d = 1.24$ g cm^{-3}). The thickness of the polymer films was 0.2 mm for PE and 0.1 mm for PES and PSF.

2.3. Irradiation

The scanning rate of ion beam (about 10 mm diameter) is 50 Hz in horizontal and 0.5 Hz in vertical axis. Ions were 10 and 20 MeV of proton, 20 and 50 MeV of He^{2+}, and 220 MeV C^{5+}, respectively. The beam current passed through the specimen is measured on the graphite beam stopper and integrated during irradiation period to obtain the total charge, which was corrected by using the current measured by the duct type Faraday cup. The current of the spot beam was about 500 nA for the proton and 50–100 nA for the heavy ion irradiation.

The stopping power of materials for each ion and penetration range were calculated by TRIM 95 code and are listed in Table 1. The stopping power is 24–28 times larger than those of 2 MeV electrons in the case of 10 MeV proton irradiation, and is 540 times larger in the 220 MeV C^{5+} irradiation.

Absorbed dose (D) in the irradiation of high energy charged particle for compounds composed of light elements like organic polymers is given by:

$$D(\text{kGy}) = S(\text{MeV cm}^2\ \text{g}^{-1}) \times Q(\mu\ \text{C cm}^{-2})/Z_{\text{inc}}$$

Table 2
Stopping power for 2MeV electron

Materials	Stopping power (MeV cm^2 g^{-1})
PE	1.77
PES	1.78
PSF	1.78

Where, S is mass stopping power of material, Z_{inc} is charge number of incident ion and Q is the fluence. The stopping powers for electron which was calculated from Seltzer and Berger method [23] are listed in Table 2.

The absorbed dose for electron (D_e) is corrected as:

$$D_e = D_c \times (S_e \text{ of polymer})/(S_e \text{ of CTA})$$

where, D_c is the dose measured by a cellulose tri-acetate (CTA) film dosimeter and S_e is mass stopping power for electron.

Table 3 shows the energy loss and the stopping power just after ions passed through the material (calculated by TRIM). In almost case, the range of ion is over six times of the sample thickness and the energy loss is 4%–9% and the difference of stopping power between the inlet and outlet in polymer film is not so large. The energy loss of the 20 MeV He^{2+}in PSF film, however, is as large as 21% of the incident energy. In this case, the averaged stopping power was used for calculation of dose. The dose rates are determined by the product of current and the stopping power of ion. For example, the dose rate for PES was 0.21 kGy s^{-1} for 10 Me V H^+, 0.14 kGy s^{-1} for 50 MeV He^{2+}, and 0.48 kGy s^{-1} for 220 Me V C^{5+}, respectively. The dose rates for PE and PSF are the same.

Electron irradiation was carried out by using 2 MeV scanning electrons from an accelerator in a vacuum chamber. To prevent temperature rising of specimen during irradiation, they were wrapped with thin aluminum foil and attached on a irradiation table having cooling water jacket by a conductive adhesive. The dose rate in the electron irradiation measured by using CTA film dosimeter was 5 kGy s^{-1}.

2.4. Measurements

Radiation effects of polymers were monitored by tensile tests, measurements of yield of gel fraction and glass transition temperature. Tensile tests were performed on JIS No 4 type dumbbell under the condition of 200 mm min^{-1} cross head speed at room temperature. Average and standard deviation of 6–7 specimens represents the data.

For gel fraction measurement, the soluble fraction was extracted by boiling xylene for PE and by chloroform at

Table 3
Energy loss of ions by passing through films and stopping power at exit

Materials	Ions and energy	Energy loss (MeV)	Stopping power at exit (MeV $cm^2 g^{-1}$)
PE thickness: 200 μm	H^+ 10 MeV	0.94	53.6
PES thickness: 100 μm	H^+ 10 MeV	0.36	44.4
	H^+ 20 MeV	0.25	24.7
	He^{2+} 50 MeV	1.86	145.4
	C^{5+} 220 MeV	15.10	974.6
PSF thickness: 100 μm	H^+ 10 MeV	0.51	45.6
	H^+ 20 MeV	0.64	25.0
	He^{2+} 20 MeV	4.16	367.4
	C^{5+} 220 MeV	12.90	1004.5

room temperature for PSF, and then yield of gel fraction and swelling ratio were determined. The heat of melting of PE and the glass transition temperature of PES and PSF were determined by differential scanning calorimetry (DSC) measurement with the heating and cooling rate of 20°C min^{-1} in nitrogen gas flow.

3. Results

The dose distribution on polymer film for ion irradiation was checked by CTA film dosimeter with 120 mm × 120 mm size (0.125 mm thickness). The distribution in the scanning 10 MeV proton spot beam on the area of 120 mm × 120 mm is shown in Fig. 2.The dot shows absorbance at the scanning point and the charts displayed in the right and upper sides show the distribution of the absorbance in *x* and *y* axis. It can be seen that the dose is uniform enough to measure mechanical property.

The tensile strength (Ts) and elongation at break (Eb) for PE in the irradiation of H^+(10 MeV) and e^- (2 MeV) are shown as a function of dose in Fig. 3. No difference in the changes of Ts and Eb are observed between proton and electron irradiations. Fig. 4a shows the change in gel fraction and swelling ratio for the same PE with dose. The gel fraction increases and swelling ratio decreases with dose, indicating that the crosslinking proceeds by proton irradiation same as that of electron. This result, however, shows that the probability of crosslinking per dose is higher in the proton than electron irradiation.

Fig. 4b shows the changes in the heat of melting (ΔH_m) of PE with dose. The ΔH_m was determined for the specimens recrystallized after irradiation. The decrease in ΔH_m is larger in the proton than that in the electron

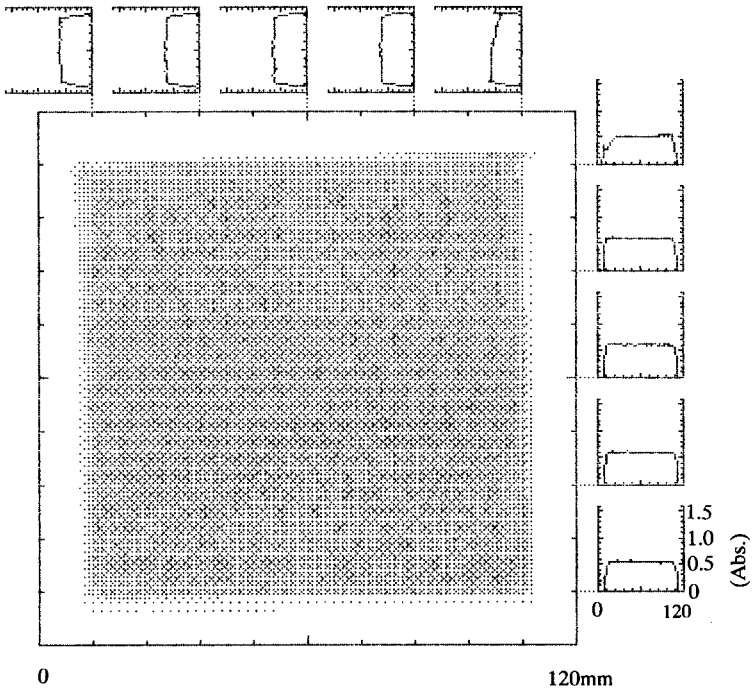

Fig. 2. Dose distribution measured by CTA film dosimeter in scanning 10 MeV proton beam to 120 × 120 mm.

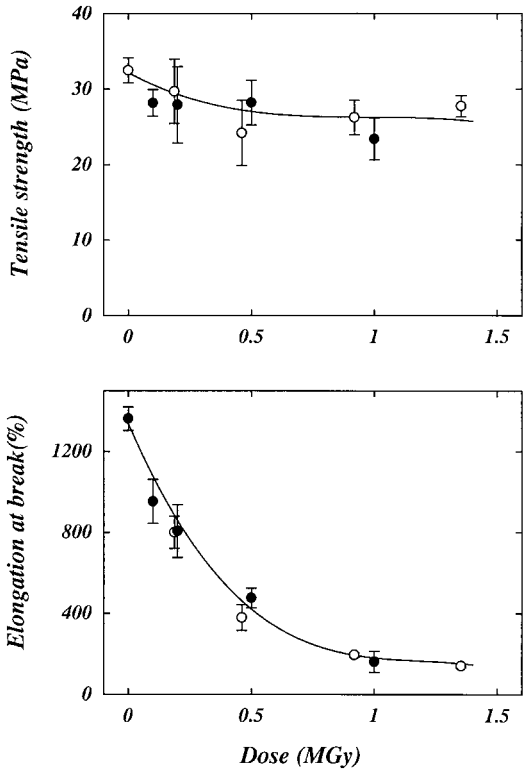

Fig. 3. Changes in tensile parameters of PE as a function of dose (○) 10 MeV proton and (●) 2 MeV electron.

irradiation, which is related to the increase in probability of crosslinking as same as the changes in gel fraction and swelling ratio.

Ts and Eb for PSF irradiated by H^+(10 MeV), H^+(20 MeV) and e^- (2 MeV) are shown in Fig. 5a and b, respectively. The change in Eb shows the same tendency among three types of radiation except for the data at 3 MGy by H^+(10 MeV), and the Ts shows some deviation in H^+(10 MeV) above 1 MGy. Fig. 5c and d show the change in Ts and Eb of PSF He^{2+}(20 MeV) and C^{5+}(220 MeV) irradiation. Both Ts and Eb show different behavior from the electron irradiation in the high dose region.

The gel fraction for PSF is shown as a function of dose in Fig. 6a. The gel formation is not observed in the electron irradiation, but the gel fraction increased above 1 MGy in the 10 MeV proton irradiation. PSF has been confirmed to undergo chain scission dominantly in the electron and γ-ray irradiation at ambient temperature [24,25], and the probability of crosslinking becomes large at high temperature [26]. The present result shows that the crosslinking proceeds in proton irradiation even at ambient temperature. Fig. 6b shows the change in glass transition temperature (T_g) of PSF with dose. The T_g in the electron irradiation decreases monotonically with dose, but the decrease of T_g in the ion irradiation is depressed. Also this fact indicates occurring of crosslinking in the ion irradiation.

The Ts and Eb for PES by H^+(10, 20 MeV) and e^- (2 MeV) irradiation is shown in Fig. 7a and b, respectively. The behavior of the changes in the tensile test is much different between proton and electron irradiation. Fig. 7c and d show the same results for PES in the heavy ion irradiation. The decrease in Eb with dose in the heavy ion irradiation becomes less than that in the 10 MeV proton irradiation.

Fig. 8 shows the radiation-induced change in T_g for PES. In the electron irradiation the T_g decreases with dose, which is originated from lowering molecular weight induced by the chain scission [24]. On the contrary, in the ion irradiation, the decrease in the T_g is extremely suppressed, indicating that the chain scission is reduced.

4. Discussion

In the case of PE, slight differences were observed on the radiation-induced changes in gel formation and heat of melting, but there is no clear difference in the changes in mechanical properties between the proton and electron

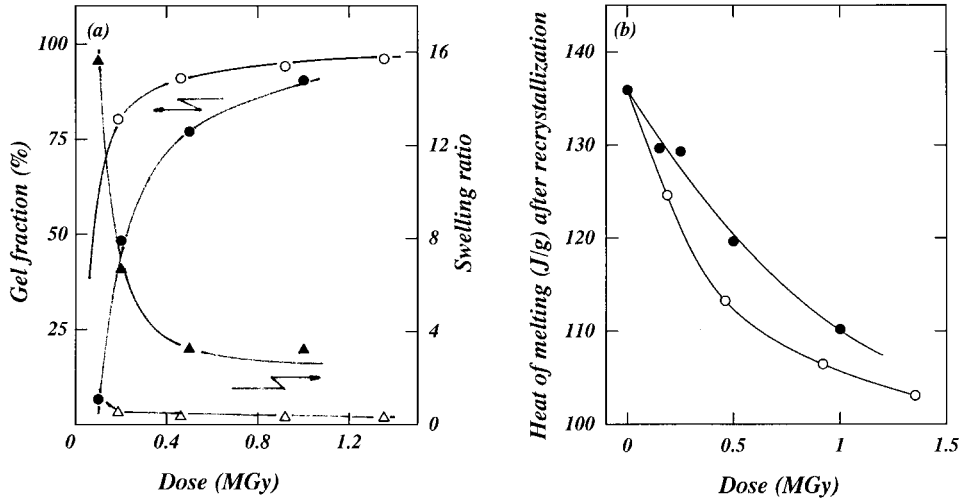

Fig. 4. Dose dependence of gel fraction, swelling ratio (a) and heat of melting (b) for PE (○)10 MeV proton and (●) 2 MeV electron.

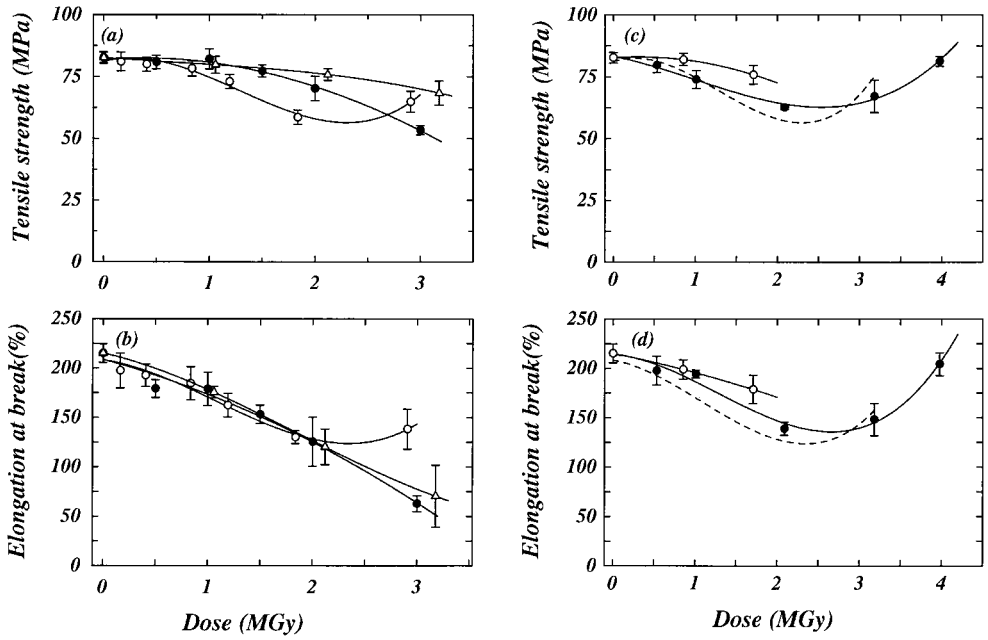

Fig. 5. Changes in tensile parameters of PSF as a function of dose, (a), (b); (○) 10 MeV proton, (△) 20 MeV proton, (●) 2 MeV electron (c), (d); (○) 220 MeV C^{5+}, (●) 20 MeV He^{2+}, (– – –) 10 MeV proton.

irradiations. The microscopic change would be too small to reflect the macroscopic property and/or distribution of the damaged sites induced by both the irradiations is apparently similar.

In the case of aromatic polymers, on the contrary, radiation-induced micro- and macroscopic property changes differed between the electron and ion irradiations. The similar LET effects in the present work have been obtained in the preliminary studies, in which the specimens were scanned against the ion beam [4,5]. There is, however, a suspicion in the previous work that the temperature of the specimens during irradiation is raised by the back heating from the sample holder because the temperature of aluminum made sample holder was not actively controlled. It can be understood easily that the temperature rising of the specimens during irradiation gives different results from irradiation under a constant temperature.

Brown and O'Donnell studied about the evolution of volatile products of PSF induced by γ-rays at 30°C, 125°C and 240°C and reported that the major product is sulfur dioxide and the *G*-Value of total gas is 0.04, 0.29 and 0.65, respectively [25]. This means that the radiolysis of diphenyl sulphone moiety increases with elevating of irradiation temperature. They also measured $G(s)/G(x)$ based on measurement of molecular weight for PSF and PES induced by the γ-ray irradiation at high temperature and reported the

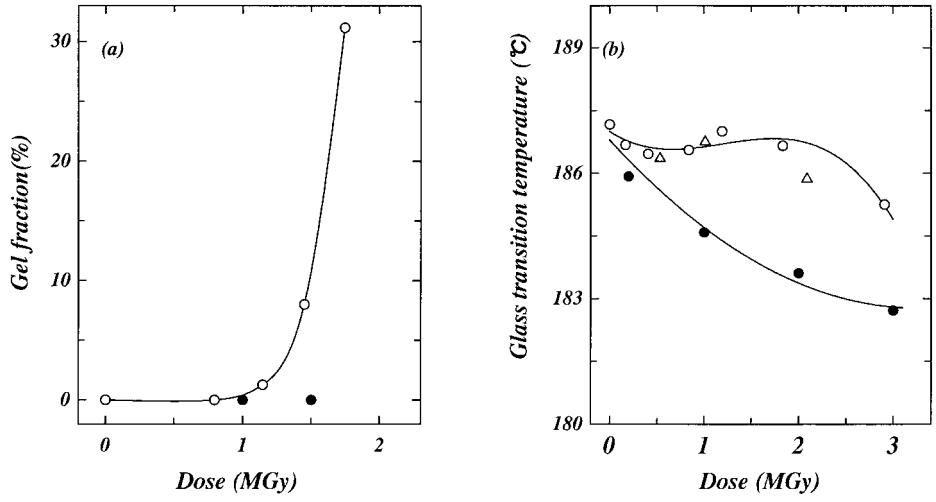

Fig. 6. Dose dependence of gel fraction (a) and glass transition temperature (b) for PSF as a function of dose, (○) 10 MeV proton, (△) 20 MeV He^{2+}, (●) 2 MeV electron.

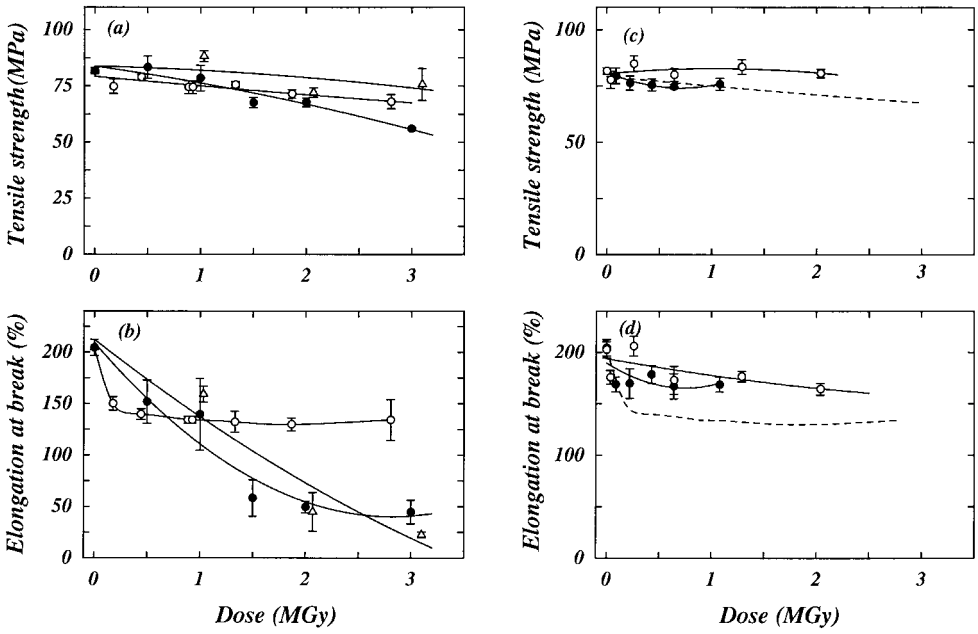

Fig. 7. Changes in of tensile parameters of PES as a function of dose, (a), (b); (○)10 MeV proton, (△) 20 MeV proton, (●) 2 MeV electron, (c), (d); (○) 220 MeV C^{5+}, (●) 50 MeV He^{2+}, (– – –) 10 MeV proton.

following results; i.e., $G(s)/G(x)$'s for PSF are 0.75 (0.03/0.04) at 30°C, 1.0 (0.05/0.05) at 80°C, 1.5 (0.30/0.20) at 125°C and 0.0(0.0/0.67) at 220°, respectively [26]. The two observations demonstrate that chain scission and crosslinking are simultaneously promoted with irradiation temperature but the degree of promotion for chain scission is higher than that for crosslinking below the T_g (ca. 185°C). It is remarkable that crosslinking only occurs above the T_g. The same result was reported for PES.

The results in the previous and present works could be interpreted by temperature rising during ion irradiation. However, the temperature of the sample holder used in the present work is controlled and it was designed as heat of 40 W/g (1 μ A of 90 MeV proton) can be removed. The estimated energy gain of the sample holder during irradiation is listed in Table 4. The result of this estimation and lower dose rate in the ion irradiation than that in the electron irradiation leads to a conclusion that the temperature rising of the specimen during irradiation is negligible. Consequently, the characteristic behavior observed in PSF and PES irradiated by ions can be concluded to be not thermal effect during irradiation.

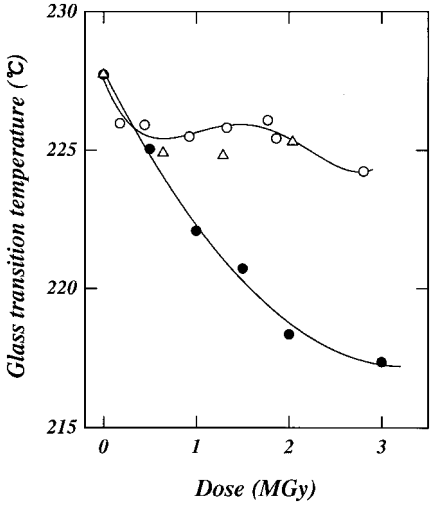

Fig. 8. Dose dependence of glass transition temperature of PSF, (△) 220 MeV C^{5+}, (○) 10 MeV proton, (●) 2 MeV electron.

In the proton irradiation, gel forms for PSF and the decrease in T_g with dose is extensively depressed for PSF and PES. These can be interpreted in terms of high-density excitation in high LET irradiation and successive increase in probability of recombination of active species. As mentioned above, PSF and PES are mainly deteriorated by chain scission at ambient temperature. The less decrement of mechanical properties per ion dose would be brought about by decrease in chain scission. Kudoh et al. has found that $G(s)$ of PMMA keeps a constant value up to the LET about 300 MeV $cm^2\ g^{-1}$ (threshold LET) and it decreases with increase of LET over the threshold LET [27]. This indicates that probability of recombination increases in very high LET region even in aliphatic polymer. It would be specific phenomena in aromatic polymers that LET effects emerge in lower LET region in PSF and PES compared with the aliphatic polymers [4–7].

It is known that excited molecules directly initiate radiation chemical reaction [10,12] in aromatic compounds. When the excited molecules are created in high density by irradiation of high LET ion, the probability of recombination would be increased. In the case of aliphatic compounds,

Table 4
Energy gain of carbon beam stopper

Ions and energy	Current of ion (nA)	Range in carbon (mm)	Energy gain (W/g)
H^+ 10 MeV	500	0.97	0.32
H^+ 20 MeV	300	3.34	0.80
He^{2+} 20 MeV	100	0.30	0.30
He^{2+} 50 MeV	100	1.45	0.15
C^{5+} 220 MeV	50	0.98	0.54

usually, reaction is initiated by radicals which are formed subsequently to excitation and/or ionization. So, probability of recombination would not be significantly enhanced by the extent of LET in this work, because active species created in the initial stage diffuses before creation of radicals. Hill et al. [8], however, reported that little difference was found between the damage to the mechanical properties of aromatic polymide film induced by 3 MeV proton and γ-rays/electron. This fact predicts that extensive studies are required on polymers with various molecular structure in order to generalize LET effect of polymer materials.

5. Summary

A chamber, which allows high-energy ions to irradiate a wide area of polymeric material uniformly was constructed. LET effects were observed on radiation-induced change in the mechanical properties in the aromatic polymer of PES and PSF. Whereas, in the case of aliphatic polymer of PE, LET effects is scarce. This result indicates that appearance or not of LET effects is owing to aromaticity of polymer, even if high-density excitation occurs.

References

[1] Wang G-H, Li X-J, Zhu Y-Z, Liu Q-S, Hu N-X, Gu X-S, Wang Q, Yu R-X, Wang T-J. Nucl Instr Meth Phys Res 1985;B 7/8:497.
[2] Coulter DR, Smith MV, Tasy F, Gupta A. J Appl Polym Sci 1985;30:1753.
[3] Wang G-H, Pan G-Q, Dou L, Yu R-X, Zhang T, Jiang S-G, Dai Q-L. Nucl Instr Meth Phys Res 1987;B 27:410.
[4] Sasuga T, Kawanishi S, Seguchi T, Kohno I. Polymer 1989;30:2024.
[5] Sasuga T, Kawanishi S, Nishii M, Seguchi T, Kohno I. Radiat Phys Chem 1991;37:135.
[6] Kudoh H, Sasuga T, Seguchi T, Katsumura Y. Polymer Commun 1996;37:3737.
[7] Kudoh H, Sasuga T, Seguchi T, Katsumura Y. Polymer 1996;37:4663.
[8] Hill DJT, Hopewell JL. Radiat Phys Chem 1996;48:533.
[9] Barr NF, Schuler RH. J Phys Chem 1959;63:808.
[10] Imamura M, Choi SU, Lichtin NN. J Am Soc 1963;85:3656.
[11] Burns WG. Trans Faraday Soc 1962;58:961.
[12] Burns WG, Parry JR. Nature 1964; 201:814.
[13] Koizumi H, Yoshida H, Namba H, Taguchi M, Kojima T. Nucl Instr Meth Phys Res 1996;B 117:431.
[14] Calcagno L, Foti G, Liccadrllo A, Puglosi O. Appl Phys Lett 1987;51:907.
[15] Calcagno L, Precolla R, Foti G. Nucl Instrm Meth Phys Res 1994; B 91:426.
[16] Le Moel A, Durauc JP, Lecomte C, Valin MT, Henriot MLE, Gressus C, Darnes C, Balanzat E, Demanet CM. Nucl Instr Meth Phys Res 1988;B 32:115.
[17] Licciardello A, Puglisi O. Nucl Instrm Meth Phys Res 1994;B 91:436.
[18] Schnabel W, Klaumunzer S, Sotobayashi H, Asmussen F, Tabata Y. Macromolecules 1984;17:2108.
[19] Aoki Y, Kouchi N, Shibata H, Tagawa S, Tabata Y. Nucl Instrm Meth Phys Res 1988;B 33:799.
[20] Schnabel W, Kalumunzer S. Radiat Phys Chem 1991;37:131.
[21] Seki S, Kanzaki K, Tagawa S, Yoshida Y, Kudoh H, Sugimoto M, Sasuga T, Seguchi T, Shibata H. Radiat Phys Chem 1997;50:423.
[22] Arakawa K, Nakamura Y, Yokota W, Fukuda M, Nara T, Agematsu T, Okumura S, Ishibori I, Karasawa T, Tanaka R, Shimizu A, Tachikawa T, Hayashi Y, Ishii K, Satoh T. Proceedings of the 13th International Conference On Cyclotron and their Applications, Vancouver, Canada, p. 119–122 (1992).
[23] Seltzer SM, Berger MJ. Radiat Phys Chem 1982;33:1189.
[24] Sasuga T, Hayakawa N, Yoshida K. Polymer 1987;28:236.
[25] Brown JR, O'Donnel JH. Appl Polym Sci 1975;19:405.
[26] Brown JR, O'Donnel JH. Appl Polym Sci 1979;23:2763.
[27] Kudoh H, Sasuga T, Seguchi T, Katsumura Y. Polymer 1996;37:2903.